Colloids and Surfaces A: Physicochemical and Engineering Aspects 631 (2021) 127698

Contents lists available at ScienceDirect

Colloids and Surfaces A: Physicochemical and Engineering Aspects

journal homepage: www.elsevier.com/locate/colsurfa

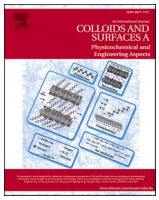

Tuning the catalytic activity of enzymes embedded in layer-by-layer assembled films

Shouwei Zhang [a], Pengyang Xin [a], Sophie Demoustier-Champagne [b,*], Alain M. Jonas [b,*]

[a] School of Chemistry and Chemical Engineering, Henan Normal University, 453007 Xinxiang, China
[b] Institute of Condensed Matter and Nanosciences – Bio and Soft Matter (IMCN/ BSMA), Université catholique de Louvain, Croix du Sud 1/L7.04.02, B1348 Louvain, la-Neuve, Belgium

ARTICLE INFO

Keywords:
Enzyme immobilization
Catalytic activity
Layer-by-Layer
Atomic force microscopy

ABSTRACT

Immobilization of enzymes on supporting materials for biocatalysis is highly desired for industrial applications, because it endows the biocatalytic platform with significant advantages compared to free enzymes, *e.g.*, easy separation, re-usability, and long-term stability. However, the possible denaturation of immobilized enzymes by the underlying substrate or crosslinking, and the limited amount of attached enzymes, often results in a low enzymatic activity. Here, we employ polyelectrolytes to assemble glucose oxidase in thick films in a layer-by-layer (LbL) way. By screening a large range of conditions, we show that the immobilized enzymes may retain their intrinsic structure and display a high activity when deposited in suitable conditions with the appropriate polycation. Moreover, the activity of formed multilayer enzyme films can be tuned depending on deposition conditions. We also demonstrate swelling of the film by the reaction medium by *in-situ* AFM measurements, with the film behaving as a hydrogel in which the enzymatic substrate can easily access the active site of enzymes immobilized all along the film. Hence, despite the complexity of protein adsorption in LbL films, conditions for stable growth of active enzymatic films of tunable activity can be found, offering a promising way to design highly active enzyme-immobilized catalytic platforms.

1. Introduction

Enzymes are natural biocatalysts with sophisticated three-dimensional structures capable of catalyzing a wide range of biochemical reactions with specific activity, offering a great promise for various industrial applications [1–3]. Generally, the industrial use of enzymes as biocatalysts requires immobilization on supporting scaffolds, because free enzymes are readily denatured and difficult to be recovered/separated from reaction products. An immobilization strategy can not only overcome these economic and operational limitations, but also bring long-term enhanced enzyme stability against heat, mechanical stirring force or organic solvents which are typically used in industrial settings [4–6].

Diverse immobilization strategies have been exploited for a variety of tasks [7], typically categorized into entrapment within a matrix and scaffold-binding [8]. Entrapment of enzymes always involves the synthesis of a matrix (*e.g.*, sol-gel, micelles and polymer capsules) in the presence of enzymes [9] whereas scaffold-binding refers to the attachment of enzymes to supporting surfaces by physical and/or chemical interactions, *e.g.*, hydrophobic, van der Waals, electrostatic interactions, and hydrogen and covalent bonds [8]. Scaffold-binding is often preferred owing to the large selection of possible supporting materials, ease of handling being another advantage. However, direct physical/chemical binding of enzymes to solid supports may cause enzyme aggregation or denaturation, resulting in a low catalytic efficiency [10]. Moreover, the undesirable release of physically-immobilized enzymes is a challenge in practical applications.

When paired with some polyelectrolytes, enzymes form complexes

* Corresponding authors.
E-mail addresses: sophie.Demoustier@uclouvain.be (S. Demoustier-Champagne), alain.jonas@uclouvain.be (A.M. Jonas).

https://doi.org/10.1016/j.colsurfa.2021.127698
Received 6 July 2021; Received in revised form 29 September 2021; Accepted 6 October 2021
Available online 13 October 2021

with them *via* physical interactions without perturbation of the secondary and tertiary structures, thus retaining their intrinsic biological activity [11–13]. The polyelectrolytes act as a glue to adhere enzymes onto the supporting surfaces. Furthermore, enzymes and polyelectrolytes can be alternately deposited in a layer-by-layer fashion, namely layer-by-layer assembly (LbL), which is a well-established technology to fabricate functional coatings on/in any supporting shape [14,15]. Its mild aqueous assembly conditions are especially suited to the immobilization of enzymatic multilayers, and the nanoscale regulation afforded over the structure of the films by assembly conditions (*e.g.*, pH, ionic strength) facilitates the fine control of the activity of LbL enzymatic films. The most exciting feature relies on its compatibility with porous supports which are ideal Supporting materials for industry thanks to their large internal surfaces.

However, the complexity of enzyme structure and the patchy nature of their surface charge distribution make the assembly of enzymes with oppositely charged polyelectrolytes complicated [16–19]. Therefore, the adsorption of protein-polyelectrolytes soluble complexes has been proposed as an alternative route for a more stable deposition [20]. Here, however, we show that robust and stable multilayers comprising glucose oxidase can be obtained by classical LbL strategy, and display a high enzymatic activity.

Glucose oxidase (GOX) is a robust enzyme with a readily available substrate, hence a good model candidate to explore enzymatic LbL assembly. Additionally, chitosan was reported to work well when paired with β-lactamase [21]. Furthermore, branched polyethyleneimine has long chain branches which are believed to tightly trap enzymes [22]. Therefore, we use glucose oxidase as model enzyme to explore the immobilization of enzymes by layer-by-layer assembly with two polycations (chitosan and branched polyethyleneimine) in different assembly conditions, and analyze their activity for optimized assembly conditions. By comparing the activity of enzyme films with different numbers of bilayers, we study the role of the terminal layer on the activity of immobilized enzymes. We find that the re-organization of immobilized enzymes by subsequent polyelectrolyte adsorption may contribute to a higher enzyme catalytic efficiency of swollen LbL enzyme films. Furthermore, the swollen structure of enzymatic LbL films in aqueous solution facilitates the free diffusion and access of substrates to the immobilized enzymes, making the LbL enzymatic films ideal coating materials for industrial applications.

2. Materials and methods

2.1. Materials

Glucose oxidase (GOX from *Aspergillus niger*, type x-s, lyophilized powder), horseradish peroxidase (HRP, type VI, lyophilized powder), branched polyethyleneimine (bPEI, M_n 60,000 g mol^{-1}, M_w *ca.* 750,000 g mol^{-1}, 50 wt% in H_2O), *o*-dianisidinedihydrochloride, 4-morpholineethanesulfonic acid (MES), acetate acid, acetate sodium (AC) and glucose were purchased from Sigma-Aldrich. Chitosan (CHI, degree of deacetylation (DD)>90%, M_w *ca.* 270,000 g mol^{-1}) was obtained from Novamatrix. 2-[4-(2-Hydroxyethyl)−1-piperazine] ethanesulfonic acid (HEPES free acid), potassium bromide (FT-IR grade, ≥99%) and dichloromethane (99.8%, for analysis) were purchased from Acros Organics. All polyelectrolytes and GOX solutions were freshly prepared at a concentration of 1.0 mg/mL either in water or in buffer at desired pH (pH range, 5.0–10.0). In these conditions, GOX has a negative charge given an isoelectric point of 4.2 [13,23,24], and PEI is positively charged [25,26]. The pH of chitosan solution was kept below 6.5, since precipitation occurs when pH exceeds 6.5 due to its low solubility which depends on the degree of protonation of lateral amine groups [27]. The zeta potentials of GOx, CHI and bPEI in different solutions were measured and summarized in Table S1. Ultrapure Milli-Q water (Millpore) with 18.2 MΩ cm resistivity was used in all experiments.

2.2. LbL assembly

Silicon was used as substrate for the LbL film construction. Briefly, prior to alternated adsorption of GOX and polycation, the silicon (1 cm×1 cm) was cleaned by immersion in a freshly prepared piranha solution (2:1 mixture of concentrated sulfuric acid and 30% hydrogen peroxide solution) for 30 min to remove contaminants as well as to maximize the negative charge density on surfaces, followed by rinsing with water and then blown dry by Ar gas. (Caution: “piranha” solution reacts violently with many organic materials and should be used with extreme care). The silicon surface was negatively charged after treatment. The multilayer films were assembled manually by repeated and sequential dipping of silicon substrates into polycation and enzyme solutions with rinsing between polyelectrolyte and enzyme depositions. In this hand-dipping procedure, the silicon substrates were first placed in a polycation solution for 15 min, followed by two rinses of 2 min each using the buffer or water which was used for adsorption solutions. Substrates were then transferred into the GOX solution following the same protocol used for the assembling of the previous layer to finalize one cycle, defined as one bilayer. At the end of the buildup process (when the desired number of bilayers was reached), the multilayered films were washed by pure water to remove the buffer salt entrapped in the film when buffer was used for the polyelectrolyte deposition, followed by drying under compressed nitrogen flow.

2.3. Spectroscopic ellipsometry

The growth evolution of LbL planar films on silicon substrates was monitored by spectroscopic ellipsometry (Uvisel, Horiba-Jobin-Yvon) by measuring their thickness in the dry state. The measurement was performed at an incidence angle of 67.2° in a wavelength range from 300 to 800 nm at 4 nm resolution. At least three measurements were performed on each sample to give an average thickness.

The collected data were analyzed by using the built-in DeltaPsi 2 software with a three-layer model. In this model, the complex index of refraction (n+jk) of bulk Si and SiO_2 were taken from the built-in database provided by the manufacturer. The thickness (d_{SiO2}) of the native SiO_2 was first measured by ellipsometry on the bare wafers just after piranha solution treatment. An average of 1.5 nm was determined by fitting on the basis of a two-layer optical model (without polymer layer on top). The SiO_2 thickness, d_{SiO2}, was subsequently fixed to 1.5 nm during the fitting of the LbL film layer in a three-layer model wherein the LbL film layer thickness and complex index of refraction are the sole unknowns, assuming a homogenous and isotropic layer. The complex index of refraction and the thickness of the LbL films were thus modeled by a Cauchy dispersion law:

$$n(\lambda) = A + \frac{B\bullet 10^4}{\lambda^2} + \frac{C\bullet 10^9}{\lambda^4}, \quad k(\lambda) = D\bullet 10^{-5} + \frac{\mathrm{E}\bullet 10^4}{\lambda^2} + \frac{\mathrm{F}\bullet 10^9}{\lambda^4} \tag{1}$$

where n, k are the refractive index and extinction coefficient, respectively, and A, B, C, E, D, F, G are Cauchy coefficients that can be determined by fitting data at each wavelength (λ). In most cases, dielectric materials are transparent in visible spectral wavelengths and become adsorbing only in the higher UV range. Therefore, a simple Cauchy transparent model was used in the visible range (560–800 nm) by setting k (λ)=0.

2.4. Atomic force microscopy (AFM)

The thickness of dried (in air) and hydrated (in aqueous solution) LbL flat enzyme films was measured with a Nanoscope VIII Multimode AFM (equipped with a fluid cell, Bruker) with peak force tapping mode (PeakFore QNM). Scratch lines were made by prep blades to uncover the silicon substrate and measure the film height (thickness). The samples were scanned in air and then in aqueous medium over an appropriate

area, which consists of film and exposed silicon substrate at a scan rate of 0.387 Hz with ScanAsyst-air and ScanAsyst-fluid probes (Bruker), respectively. Before AFM measurements in aqueous solutions in the fluid cell, a small droplet of solution was placed on the samples that were previously scanned in air and leave at rest for 40 min to reach dynamic equilibrium. Collected images (20×20 μm^2) were used to compute the film thickness by statistical analysis after flattening the substrate area (film area excluded) using 1st order polynomials in a line-by-line type in X direction. The root-mean-square (RMS) roughness was reported for 10×10 μm^2 images after flattening the whole image by using zero order polynomials in a line-by-line scan in the X direction. All acquired data were analyzed by home-made programs. The swelling degree (SD) of LbL films on silicon in aqueous solutions was calculated as follows:

$$SD = \frac{d_{wet} - d_{dry}}{d_{dry}}$$

where d_{dry} and d_{wet} are the film thicknesses measured in air and in aqueous solution, respectively. The scanned areas in air and in fluid are exactly identical in order to avoid the influence of variation in film thickness at different locations of the sample.

2.5. FTIR measurements and analysis

Fourier transform infrared (FTIR) spectra were collected at 8 cm^{-1}resolution (128 passes) on an FTIR spectrometer (Nicolet Nexus 870, Thermo Scientific). For free glucose oxidase, a standard KBr disk was prepared. As for the polyethyleneimine aqueous viscous solution, it was simply deposited over an IR-transparent support (ZnSe crystal), and the spectrum acquired with a Continuμm IR microscope (Nicolet) in transmission. For $(bPEI/GOX)_n$ films or GOX adsorbed on silicon substrates, the spectra were recorded directly in transmission with a freshly prepared bare silicon as background, whereas Infrared reflection-absorption spectroscopy (IRRAS) was exploited to detect the layer of bPEI or GOX adsorbed on Au-coated silicon with the help of a smart SAGA accessory.

2.6. Enzyme activity

The activity of the enzyme was measured spectrophotometrically (Agilent Cary 50) by monitoring the production of soluble oxidized *o*-dianisidine (yellow-orange), which is generated by the oxidation of reduced *o*-dianisidine (colorless) in the presence of peroxidase (POD) and hydrogen peroxide (H_2O_2). The H_2O_2 is the product of oxidation of glucose by oxygen, catalyzed by glucose oxidase. To measure the activity of planar enzymatic films grown on flat silicon substrates, a piece of enzyme-loaded silicon square (11 mm×11 mm) was glued using double-sided tape in a well, with the rough surface of the Si wafer sticking on the base of the well to exclude the contribution to the measured activity of the film of enzyme deposited on this rough surface; then, 2.00 mL of a 0.3 mM *o*-dianisidine dihydrochloride solution in 50 mM sodium acetate buffer (pH 5.5), and 0.20 mL of a horseradish peroxidase (HRP) solution (containing approximately 60 units/mL) were poured into the well (12 well cell culture plate) containing the enzyme-modified silicon square, and air-equilibrated. 0.50 mL of a 3.0 mM glucose solution was then added to the well and the increase in absorbance at 460 nm (maximum absorption) of the solution was recorded at room temperature every two minutes immediately after mixing, for 20 min during which continuous shaking was applied (KS-15 shaker, Edmund Bühler GmbH). The enzyme activity was here defined as the initial rate of the coupled reaction, *i.e.*, the initial increase per min of the absorbance at 460 nm, $\Delta A_{460\ nm}$/min.

3. Results and discussion

3.1. Construction of enzyme-containing multilayer film

LbL assembly on the basis of weak interactions between polyelectrolytes is not always feasible [28,29], depending on the nature of polyelectrolytes and the assembly conditions, typically pH and ionic strength of polyelectrolyte solutions, and use or not intermediate drying steps [30,31]. In particular, the buildup of protein multilayer films *via* the assembly of various proteins with oppositely charged polyelectrolytes is really a challenge [17,20,23,32,33], owing to the complexity of their structure and the patchy nature of their distribution of surface charge. As reported previously [13,34,35], several polycations, for instance, chitosan (CHI), and branched polyethyleneimine (bPEI), work well when paired with enzymes. Herein, the buildup of GOX alternating with chitosan (Fig. 1A) or branched polyethyleneimine (bPEI) (Fig. 1B) films on planar surfaces in various assembly conditions was explored by spectroscopic ellipsometry. The thickness evolution of the multilayer films was monitored in dry conditions, providing a preliminary insight into the growth behavior of protein films. To make sure that GOX enzyme exhibits a globally negative charge in solution, the pH of the GOX solution was always adjusted at a value higher than GOX isoelectric point (4.2) [13,23,24]. For chitosan, with a pKa=6.0–6.5 [36,37], a pH beyond 6.5 reduces sharply the positive charge density along chitosan chains due to the deprotonation and consequently decreases its solubility, resulting in flocculation. To avoid precipitation, the pH of the chitosan solution was thus limited to the 5–6.5 range, and the assembly of CHI with GOX was always performed in this pH range. However, for bPEI/GOX films, the assembly was performed at a pH beyond 6.5 to maximize the surface negative charge density of the globular GOX enzymes and strengthen the electrostatic interactions.

Under all tested conditions, similar fluctuation trends in the thickness of CHI/GOX films were observed (Fig. 1C). The thickness fluctuation is also shown to depend on the nature of the outermost layer (GOX or CHI), suggesting that the GOX previously adsorbed over a chitosan layer is heavily released when the next CHI layer is deposited, although low buffer concentrations and high pHs increase the amount of adsorbed GOX at each step. For instance, a 4 nm thick GOX layer is adsorbed over a CHI layer in 50 mM acetate buffer (pH 5.1), while its thickness increases to 8 nm in 10 mM MES buffer (pH 6.5), close to the spherical diameter of GOX, 60–80 Å [23,38,39]. However, a heavy release of adsorbed GOX upon subsequent CHI deposition is observed, regardless of the amount of previously absorbed GOX over the CHI layer, leading to a limited growth in 10 mM MES buffer (pH 6.5) and even non-growth of films in a 50 mM buffer solution. To check the possibility of applying intermediate drying step to improve the stability of the enzyme layer against the subsequent deposition of a chitosan layer, as well as increasing the amount of GOX adsorbing over a pre-dried chitosan layer, a series of samples with different numbers of (CHI/GOX) bilayers were dried and further immersed into polyelectrolyte solutions (CHI or GOX) (Fig. S1A). GOX and CHI-terminated films were incubated in CHI and GOX solutions, respectively. A similar release and adsorption of enzymes was observed on the samples which experienced drying, revealing that drying neither enhanced the stability of the enzyme layer nor increased enzyme adsorption.

For bPEI/GOX films, the situation is totally different. In most tested conditions, growth was generally observed, characterized by an increase in average film thickness (Fig. 1D). Depending on assembly conditions, a tiny decrease in thickness was however detected due to a limited desorption of GOX when bPEI is deposited over the precedingly-adsorbed GOX layer, in agreement with AFM (Fig. S2) and FTIR measurements (Fig. 2A and S3). Higher buffer concentrations and lower assembly pHs gave rise to a larger enzyme release, indicating that lower ionic strengths and higher pHs facilitate the buildup of LbL enzymatic films, resulting in a faster LbL growth. At low ionic strength, unlike for the CHI/GOX pair, the rinsing medium plays a signification role in film

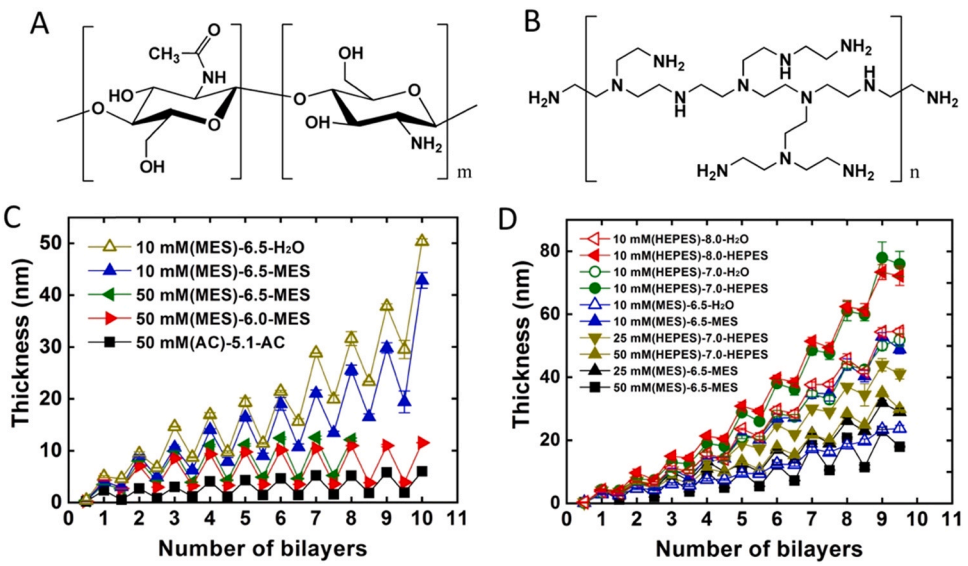

Fig. 1. Molecular structures of chitosan (A) and branched polyethyleneimine (B). LbL growth evolutions determined by ellipsometry *versus* the number of bilayers deposited on flat silicon substrates for CHI/GOX (C) and bPEI/GOX (D) films under various deposition conditions. Integral numbers of bilayers correspond to the deposition of a GOX layer; half-integral numbers to the deposition of a polycation layer. Acetate (AC) buffer (pH 5.1), MES buffer (pH 6.5) and HEPES buffer (pH 7.0, or 8.0) were used for the LbL assembly. The sample denomination in (C, D) is (concentration and solvent used for the deposition)-(solvent pH)-(solvent used for rinsing).

growth. Using a buffer medium instead of pure water for intermediate washing steps yielded thicker enzyme LbL films. The slower growth when pure water was used for intermediate rinsing steps might be attributed to the reorganization of the previously adsorbed chitosan layer upon exposure to a medium of different pH, consequently affecting subsequent GOX accumulation. No significant difference was observed between LbL assembly at pH 7.0 and 8.0 when 10 mM HEPES buffer was used for the buildup, suggesting further increase in solution pH made minor contribution.

The buildup process resulting from alternated deposition of GOX and polycations (CHI, bPEI) in pure water was investigated as well. A thickness of *ca.* 300 nm could be reached for 9.5-bilayer films, regardless of the polycation used (Fig. S1B). In this case, the enzymes may penetrate in the previously formed film, resulting in an exponential growth. A slight removal of adsorbed enzyme occasionally occurred during polycation deposition, indicating that pure water (low ionic strength) not only promotes GOX deposition over the previous polycation layer but also prevents the dissolution of GOX-polycation complexes.

However, when the pH of GOX (initial pH, 7.2) and bPEI (initial pH, 10) solutions were adjusted to 6.5, the growth evolution (rinsed in pure water without NaCl) was totally different, exhibiting much slower increment in thickness per bilayer. This is primarily due to the moderate amount of GOX adsorbed on previous bPEI layers, 10 nm of GOX layer compared to 50 nm (when the pH of GOX and bPEI solutions were 7.2 and 10.2, respectively); however, very little GOX release is observed when the multilayers are exposed to the bPEI solution at pH 6.5. One should be aware of the fact that, apart from the pH change by addition of HCl, the increase in ionic strength of the bPEI solution resulting from the pH adjustment also play important role in LbL film growth (Fig. S1B). The amount of absorbed GOX depends on the properties of the previous bPEI layer which depends on the pH and ionic strength of the bPEI solution. The contact angles of bPEI/GOx-terminated films prepared in polyelectrolyte solutions with different pHs were measured (Fig. S5). bPEI layer deposited at higher pH has a slightly smaller contact angle, indicating that pH of polyelectrolyte can moderately regulate the surface wettability of films. The properties of the underlying layer are indeed crucial for the sequential adsorption of oppositely charged polyelectrolytes [40].

These observations demonstrate that high pH and low ionic strength facilitate LbL enzymatic film growth. They also show the utmost sensitivity of the LbL growth process to minute variations of assembly conditions, which is typical of protein LbL assembly and results from the complex and patchy distribution of surface potential of proteins. Nevertheless, despite this complexity, it is possible to find proper deposition conditions by exploring systematically the range of possible conditions. To avoid the possible denaturation of GOX enzyme during the assembly while ensuring a large amount of enzyme in the films, bPEI/GOX enzyme films built in 10 mM HEPES buffer (7.0) were selected for further investigation.

3.2. *Redispersion of immobilized enzyme by subsequent bPEI adsorption for higher activity*

The activity of GOX planar films assembled in 10 mM HEPES buffer at pH 7.0 was thus measured. A regular increase in the activity of films with increasing number of bilayers was observed (Fig. 2A), revealing the accumulation of enzyme on the silicon wafer in a layer by layer fashion, as evidenced by the thickness evolution. However, there exists a transition in activity at around four bilayers, at which point the film enters into a faster and stable growth region (Fig. 2A). This transition phenomenon occurring during growth is commonly observed, because the film usually takes several bilayers to fully eliminate the influence of the substrate and establish a stable growth [41].

Of interest is the low activity of films below four bilayers (thickness lower than 13 nm), while a significant amount of GOX is observed by infrared spectroscopy (Fig. 2A). For instance, as for $(bPEI/GOX)_2$ film, a monolayer of GOX (complexed with bPEI) is present on the silicon substrate (7.7 nm), approximately identical to the GOX enzyme size [38, 39]. A full coverage of GOX enzymes over silicon substrates for 2-bilayer film was observed by AFM (Fig. S6). This GOX monolayer yielded 0.00029 of increment in activity, which is at least 100 times lower than the activity per additional GOX layer measured in the second linear region of Fig. 2A. This very low increment in activity per amount of adsorbed GOX in the first cycles of deposition may be ascribed to the denaturation of the enzyme adsorbed close to the substrate at the initial stage of buildup process. This unfavorable denaturation by the bare hard substrate may be eliminated by first constructing a buffering multilayer film that can serve as a soft cushion for deposition of enzyme films, e.g (polyacrylic acid) (PAA)/bPEI multilayer film.

We also used IR spectroscopy to identify the secondary structure of the assembled enzymes (Fig. 2B). Intense bands in the amide I and II regions were observed in all spectra. Compared to the IR spectrum of free GOX, specifically the amide I and II bands at about 1654 and 1541 cm^{-1}, no significant changes in either position or band shape were observed for 3, 4 and 6-bilayer films, suggesting that the GOX component retains its native secondary structure. However, a slight red shift of

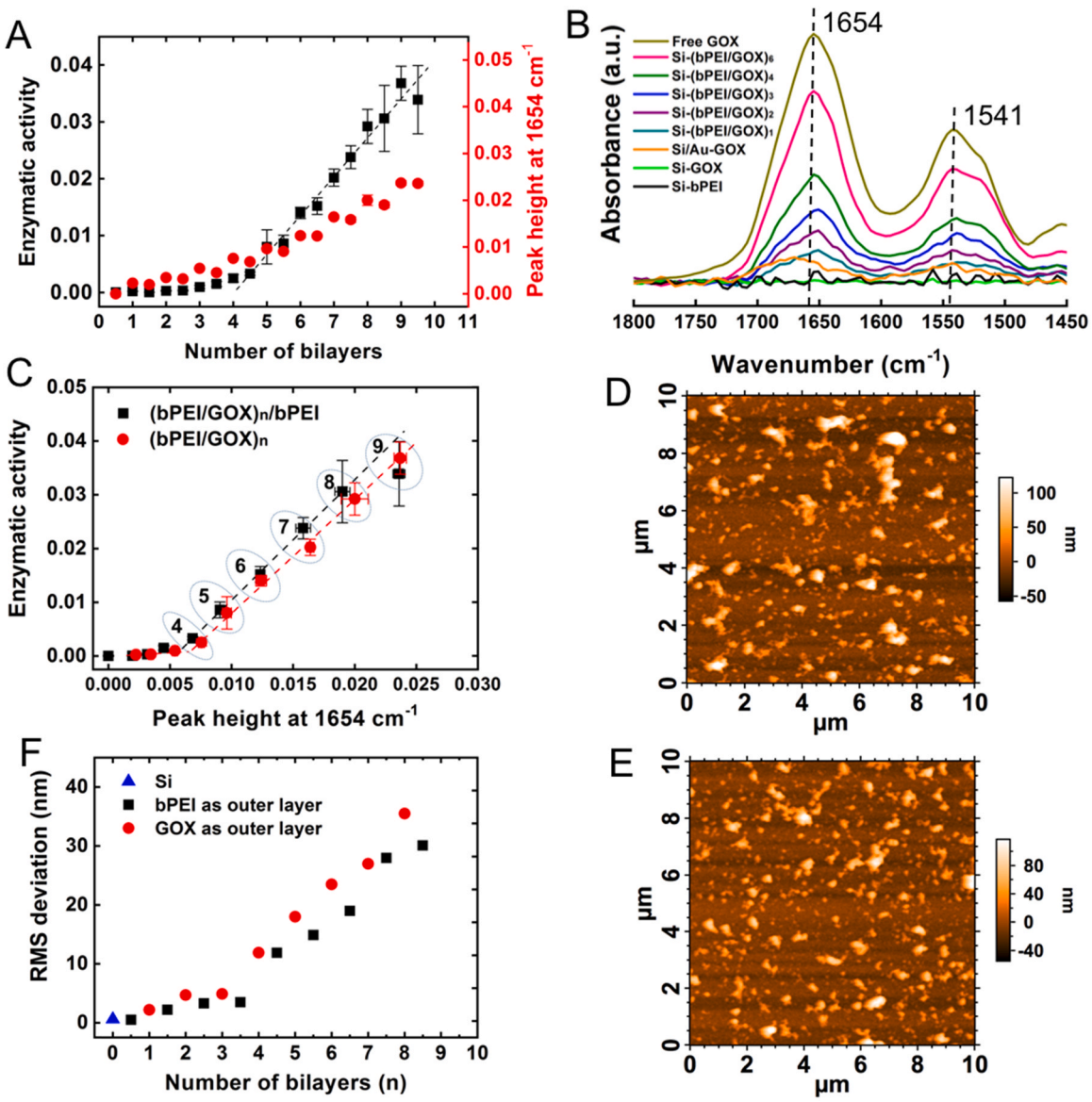

Fig. 2. (A) Activity (left axis) and GOX absorbance intensity at 1654 cm^{-1} in FTIR spectra (right axis) of planar films; The content of GOX in planar films is supposed to be proportional to the absorbance of GOX at 1654 cm^{-1} (amide I) measured by FTIR transmission on the basis of Beer-Lambert law. The peak height at 1654 cm^{-1} was derived from Fig. S3. (B) FTIR spectra of free GOX enzyme, and 1-bilayer, 2-bilayer, 3-bilayer, 4-bilayer and 6-bilayer GOX films deposited on substrates. (C) Plots of activity against GOX content for $(bPEI/GOX)_n$ films. The red filled circles represent the films $(bPEI/GOX)_n$ with GOX as ending layer, while black solid squares denote the $(bPEI/GOX)_n$/bPEI films as a results of bPEI deposition on $(bPEI/GOX)_n$ films. The number n is indicated in dotted ellipses. (D, E) Topography of $(bPEI/GOX)_6$ (D) and $(bPEI/GOX)_{6.5}$ (E) films in air. (F) RMS roughness (in air) of flat films deposited on silicon wafers at different number of bilayers. RMS values were calculated from corresponding images (10×10 μm^2) shown in Fig. S4. Error bars in (A, C) are derived from three independent experiments. Dashed lines are drawn to guide the eye.

the amide I band and a pronounced change in amide II band shape for 1- and 2-bilayer films confirms that the incorporated GOX close to silicon is denatured [42,43], consequently leading to a lower activity of very thin films.

Starting from four bilayers, the activity increases strongly and linearly, regardless of GOX or bPEI being the outermost layer (Fig. 2A); however, the GOX content (in terms of GOX IR absorbance at 1654 cm^{-1}) of the GOX-terminated films was reduced slightly by the sequential deposition of the bPEI layer owing to a tiny desorption of previously adsorbed GOX, which is in accordance with the thickness evolution. To make it clearer, we plotted the activity against the content of GOX in flat films (Fig. 2C). A tiny increment in activity due to the deposition of bPEI layer is observed, despite the associated tiny decrease of film thickness and IR-measured GOX content. This suggests that, upon exposure to the bPEI solution, a small structural reorganization of the adsorbed enzyme layer takes place, without important removal of adsorbed enzymes. We then used AFM to probe the layer texture before and after bPEI deposition on the surface. As shown in Fig. 2D, E and S4, enzyme aggregates were observed on the surface, more pronounced for films with four and more bilayers. Furthermore, enzyme aggregates became generally smaller upon subsequent adsorption of bPEI over the GOX layer, as evidenced by a smoother bPEI-terminated surface (Fig. 2F). Together with the detected increase of activity, we hypothesize that bPEI adsorption results in improved enzyme dispersion (Fig. 3); this improves the catalytic efficiency of immobilized enzymes, leading to a higher activity even though a tiny amount of enzyme was released by this reorganization. Moreover, a bPEI coating on GOx layer can improve the enzyme stability against pH or high temperature that may

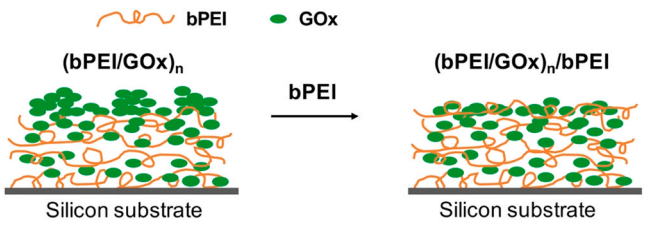

Fig. 3. Schematic illustrations of the redispersion of previously adsorbed enzymes by the subsequent deposited bPEI. The adsorption of GOX on bPEI layer results in a significant increase in film thickness because of the clustering of enzymes on the surface. Once being in contact with a bPEI solution, the bPEI chains would interact with enzymes on the surface and penetrate the enzyme layer with some enzyme release into solution, leading to a better dispersion of the enzymes.

cause enzyme denaturation [13].

However, in our case, this reorganization by following adsorption of bPEI was achieved to a limited extent, because it is difficult to redisperse previously adsorbed enzyme layers by subsequent polyelectrolyte adsorption without enzyme removal. The distribution of enzymes on the surface might be tuned using different assembly conditions.

3.3. *Stable swollen film structure for non diffusion-controlled bioreactions*

In a fixed test condition, the actual activity of enzyme films is affected by many factors, including the amount and distribution of immobilized enzymes, whether the immobilized enzymes are denatured or not, and the permeability of films to reaction substrate and products. Typically, when placed in an aqueous solution where enzymatic reactions take place, LbL films usually swell due to the uptake of solution, and the swelling depends on the film structure as well as solution

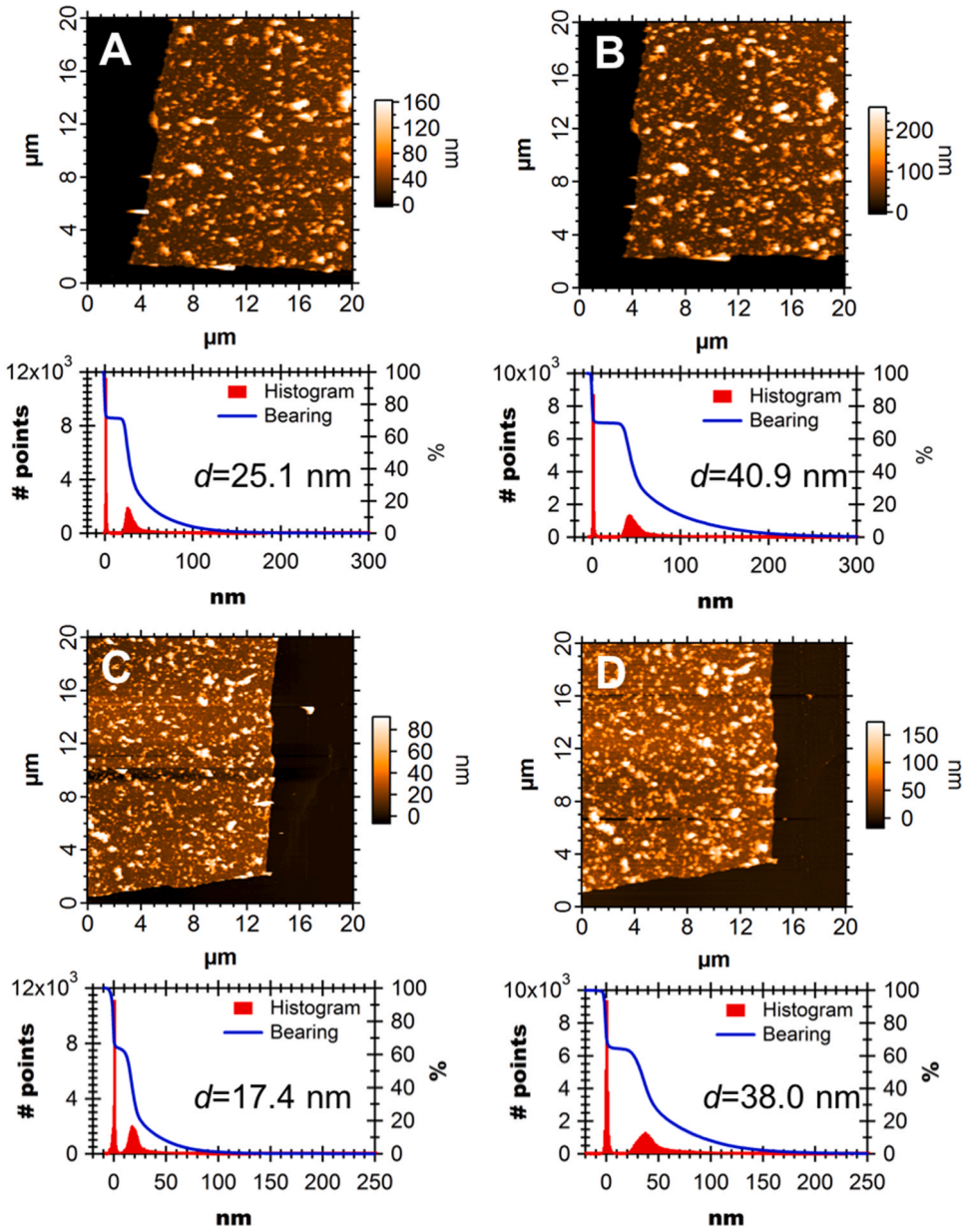

Fig. 4. *In-situ* AFM measurement of swelling of enzymatic films in solution. Dry (A, C) and hydrated thickness in 50 mM acetate buffer (pH 5.5) (B) and fructose (D) of a 6.5-bilayer film prepared in 10 mM HEPES at pH 7.0. The fructose was added in 50 mM sodium acetate buffer at pH 5.5. The thickness *d* was obtained by statistical analysis (histogram graphs shown beneath each AFM image).

parameters (*e.g.*, pH, ionic strength and type of solute) [44–46].

In our case, the enzymatic reaction is performed in 50 mM acetate buffer (pH 5.5), conditions for which free GOX enzymes exhibit the highest activity. In order to evaluate the swelling behavior of the films under these conditions, the dry and wet thicknesses of flat 6.5-bilayer films in 50 mM acetate buffer (pH 5.5) was measured by AFM (Fig. 4A, B). To eliminate the contribution of the variation in film thickness from one spot to another in one sample or from one sample to another, the thickness in dry and subsequent wet states was probed at exactly the same position from same sample, as shown in Fig. 4. Identical surface features of films were observed in the dry and wet states with only difference in the size of dots present on the film surface. In the wet state, these dots appear larger than in the dry state, showing that the film is well swollen by the aqueous media. The average dry thickness of a flat 6.5-bilayer film was determined by ellipsometry to be *ca.* 20±3 nm. Here, we used AFM to measure *in situ* the dry and hydrated thicknesses to eliminate the influence of the variation in film thickness from sample to sample. By measuring the wet thickness of the same film, the swelling degree in 50 mM acetate buffer (pH 5.5) was found to be *ca.* 64% (Table 1). In order to find out whether the diffusion of glucose to the film is a limiting step or not in 50 mM acetate buffer (pH 5.5), we used a small inactive model molecule, fructose, to swell the film further. GOX has no activity towards fructose, avoiding the enzymatic reaction during the AFM measurements (Fig. 4C, D). Indeed, fructose present in solution induces a further swelling of the LbL film with a swelling degree of *ca.* 117% (Table 1), because of the additional osmotic forces exerted on the enzymatic films. However, further swelling by fructose solutes does not increase the activity of the flat film further [11], suggesting that the swollen structure of LbL films in an aqueous solution provides already a very easy diffusion pathway for the glucose substrate and products, better than other enzyme-immobilized systems, *e.g.*, entrapment networks. Therefore, LbL assembly immobilization strategy offers a smart way for the immobilization of bioactive components for bioapplications.

4. Conclusions

In summary, enzymatic layer-by-layer films were successfully constructed by optimizing the assembly conditions including pH, ionic strength, nature of polycation and assembly protocol. High pH and low ionic strength promote the buildup of GOX-comprising multilayer films; bPEI appears particularly well-suited for the growth of stable enzyme-based films. The activity of enzymatic films with different number of bilayers was also tested, showing two distinct regimes with a transition at around four bilayers. The denaturation of immobilized enzymes by contact with the substrate accounts for the weak enzymatic activity of films in first regime. When the growth of the film enters the faster and stable second regime, the activity increases linearly along with the number of bilayers. PEI-terminated films have an identical activity as GOX-terminated films even though they contain less enzymes, suggesting enzymes in PEI-terminated films have higher catalytic efficiency. This was attributed to an improved distribution of immobilized enzymes following the adsorption of bPEI, leading to a slightly better catalytic efficiency. Moreover, we demonstrated that the stable swollen film structure in aqueous solution enables the free diffusion of the substrate to the immobilized enzymes, which is a great advantage. Globally, our findings provide tools for the rational design of enzyme-containing films, showing that active films obtained by LbL hold opportunities for bio-applications.

CRediT authorship contribution statement

Shouwei Zhang: Conceptualization, Methodology, Investigation, Writing – original draft. **Pengyang Xin:** Data investigation. **Sophie Demoustier-Champagne:** Conceptualization, Supervision, Writing – review & editing. **Alain M. Jonas:** Conceptualization, Supervision, Writing – review & editing.

Table 1
Swelling degree of 6.5-bilayer planar films in different media measured by AFM.

Medium	Dry thickness[c] (nm), d_{dry}	Wet thickness[d] (nm), d_{wet}	Swelling degree (%)
Acetate buffer[a]	25.1±4.7	40.9±6.0	62.9±2.5
Fructose in buffer[b]	17.4±3.6	38.0±7.6	117.4±0.3

[a] 50 mM sodium acetate, pH 5.5.
[b] Fructose in 50 mM sodium acetate, pH 5.5.
[c] The thicknesses measured on as-prepared films by AFM in air before samples were imaged in fluid.
[d] The thicknesses of the identical samples in aqueous conditions.

Declaration of Competing Interest

The authors declare that they have no known competing financial interests or personal relationships that could have appeared to influence the work reported in this paper.

Acknowledgements

This work was financially supported by the Belgian Science Policy (IAP P6/27), and the Belgian Fund for Scientific Research (FNRS). This work was also supported by National Natural Science Foundation of China (U2004188), the Natural Science Foundation of Henan Province (212300410053), and the Special Project for Fundamental Research in University of Henan Province (21ZX005).

Appendix A. Supporting information

Supplementary data associated with this article can be found in the online version at doi:10.1016/j.colsurfa.2021.127698.

References

[1] O. Kirk, T.V. Borchert, C.C. Fuglsang, Industrial enzyme applications, Curr. Opin. Biotechnol. 13 (4) (2002) 345–351.
[2] J.M. Choi, S.S. Han, H.S. Kim, Industrial applications of enzyme biocatalysis: current status and future aspects, Biotechnol. Adv. 33 (7) (2015) 1443–1454.
[3] J. Chapman, A. Ismail, C. Dinu, Industrial applications of enzymes: recent advances, techniques, and outlooks, Catalysts 8 (6) (2018) 238.
[4] S. Demirci, N. Sahiner, Superporous neutral, anionic, and cationic cryogel reactors to improved enzymatic activity and stability of α-Glucosidase enzyme via entrapment method, Chem. Eng. J. 409 (2021), 128233.
[5] M.N. Morshed, N. Behary, N. Bouazizi, J. Guan, V.A. Nierstrasz, An overview on biocatalysts immobilization on textiles: preparation, progress and application in wastewater treatment, Chemosphere 279 (2021), 130481.
[6] S. Datta, R. Veena, M.S. Samuel, E. Selvarajan, Immobilization of laccases and applications for the detection and remediation of pollutants: a review, Environ. Chem. Lett. 19 (1) (2020) 521–538.
[7] A.A. Homaei, R. Sariri, F. Vianello, R. Stevanato, Enzyme immobilization: an update, J. Chem. Biol. 6 (4) (2013) 185–205.
[8] R.A. Sheldon, Enzyme immobilization: the quest for optimum performance, Adv. Synth. Catal. 349 (8–9) (2007) 1289–1307.
[9] P. Walde, S. Ichikawa, Enzymes inside lipid vesicles: preparation, reactivity and applications, Biomol. Eng. 18 (4) (2001) 143–177.
[10] D.-M. Liu, J. Chen, Y.-P. Shi, Advances on methods and easy separated support materials for enzymes immobilization, TrAC Trends Anal. Chem. 102 (2018) 332–342.
[11] S. Zhang, S. Demoustier-Champagne, A.M. Jonas, Quantitative collection and enzymatic activity of glucose oxidase nanotubes fabricated by templated layer-by-layer assembly, Biomacromolecules 16 (8) (2015) 2382–2393.
[12] F. Caruso, C. Schüler, Enzyme multilayers on colloid particles: assembly, stability, and enzymatic activity, Langmuir 16 (24) (2000) 9595–9603.
[13] M. Onda, K. Ariga, T. Kunitake, Activity and stability of glucose oxidase in molecular films assembled alternately with polyions, J. Biosci. Bioeng. 87 (1) (1999) 69–75.
[14] P. Bertrand, A. Jonas, A. Laschewsky, R. Legras, Ultrathin polymer coatings by complexation of polyelectrolytes at interfaces: suitable materials, structure and properties, Macromol. Rapid Commun. 21 (7) (2000) 319–348.
[15] S. Zhang, F. Xia, S. Demoustier-Champagne, A.M. Jonas, Layer-by-layer assembly in nanochannels: assembly mechanism and applications, Nanoscale 13 (16) (2021) 7471–7497.
[16] A. Yu, Z. Liang, F. Caruso, Enzyme multilayer-modified porous membranes as biocatalysts, Chem. Mater. 17 (1) (2005) 171–175.

[17] P. Pescador, I. Katakis, J.L. Toca-Herrera, E. Donath, Efficiency of a bienzyme sequential reaction system immobilized on polyelectrolyte multilayer-coated colloids, Langmuir 24 (24) (2008) 14108–14114.
[18] Y. Lvov, K. Ariga, I. Ichinose, T. Kunitake, Assembly of multicomponent protein films by means of electrostatic layer-by-layer adsorption, J. Am. Chem. Soc. 117 (22) (2002) 6117–6123.
[19] A. Vander Straeten, D. Lefevre, S. Demoustier-Champagne, C. Dupont-Gillain, Protein-based polyelectrolyte multilayers, Adv. Colloid Interface Sci. 280 (2020), 102161.
[20] A. Vander Straeten, A. Bratek-Skicki, A.M. Jonas, C.A. Fustin, C. Dupont-Gillain, Integrating proteins in layer-by-layer assemblies independently of their electrical charge, ACS Nano 12 (8) (2018) 8372–8381.
[21] D.G. Ramírez-Wong, C. Coelho-Diogo, C. Aimé, C. Bonhomme, A.M. Jonas, S. Demoustier-Champagne, Effects of geometrical confinement in membrane pores on enzyme-based layer-by-layer assemblies, Appl. Surf. Sci. 338 (2015) 154–162.
[22] X. Qu, G. Lu, E. Tsuchida, T. Komatsu, Protein nanotubes comprised of an alternate layer-by-layer assembly using a polycation as an electrostatic glue, Eur. Chem. J. 14 (33) (2008) 10303–10308.
[23] Y. Lvov, K. Ariga, I. Ichinose, T. Kunitake, Assembly of multicomponent protein films by means of electrostatic layer-by-layer adsorption, J. Am. Chem. Soc. 117 (22) (1995) 6117–6123.
[24] C. Schüler, F. Caruso, Preparation of enzyme multilayers on colloids for biocatalysis, Macromol. Rapid Commun. 21 (11) (2000) 750–753.
[25] J. Suh, H.J. Paik, B.K. Hwang, Ionization of poly(ethylenimine) and poly (allylamine) at various pH′s, Bioorg. Chem. 22 (3) (1994) 318–327.
[26] J. Nagaya, M. Homma, A. Tanioka, A. Minakata, Relationship between protonation and ion condensation for branched poly(ethylenimine), Biophys. Chem. 60 (1–2) (1996) 45–51.
[27] G. Skjåk-Bræk, H. Grasdalen, O. Smidsrød, Inhomogeneous polysaccharide ionic gels, Carbohydr. Polym. 10 (1) (1989) 31–54.
[28] S.A. Sukhishvili, E. Kharlampieva, V. Izumrudov, Where polyelectrolyte multilayers and polyelectrolyte complexes meet, Macromolecules 39 (26) (2006) 8873–8881.
[29] N. Nuraje, R. Asmatulu, R.E. Cohen, M.F. Rubner, Durable antifog films from layer-by-layer molecularly blended hydrophilic polysaccharides, Langmuir 27 (2) (2011) 782–791.
[30] P. Bertrand, A. Jonas, A. Laschewsky, R. Legras, Ultrathin polymer coatings by complexation of polyelectrolytes at interfaces: suitable materials, structure and properties, Macromol. Rapid Commun. 21 (7) (2000) 319–348.
[31] J.M. Lourenco, P.A. Ribeiro, A.M. Botelho do Rego, M. Raposo, Counterions in layer-by-layer films – influence of the drying process, J. Colloid Interface Sci. 313 (1) (2007) 26–33.
[32] F. Caruso, C. Schüler, Enzyme multilayers on colloid particles: assembly, stability, and enzymatic activity, Langmuir 16 (24) (2000) 9595–9603.
[33] A. Yu, Z. Liang, F. Caruso, Enzyme multilayer-modified porous membranes as biocatalysts, Chem. Mater. 17 (1) (2005) 171–175.
[34] D.G. Ramírez-Wong, C. Coelho-Diogo, C. Aimé, C. Bonhomme, A.M. Jonas, S. Demoustier-Champagne, Effects of geometrical confinement in membrane pores on enzyme-based layer-by-layer assemblies, Appl. Surf. Sci. 338 (2015) 154–162.
[35] X. Qu, G. Lu, E. Tsuchida, T. Komatsu, Protein nanotubes comprised of an alternate layer-by-layer assembly using a polycation as an electrostatic glue, Chem. Eur. J. 14 (33) (2008) 10303–10308.
[36] Q.Z. Wang, X.G. Chen, N. Liu, S.X. Wang, C.S. Liu, X.H. Meng, C.G. Liu, Protonation constants of chitosan with different molecular weight and degree of deacetylation, Carbohydr. Polym. 65 (2) (2006) 194–201.
[37] R. Riva, H. Ragelle, A. des Rieux, N. Duhem, C. Jérôme, V. Préat, Chitosan and chitosan derivatives in drug delivery and tissue engineering, Adv. Polym. Sci. 244 (2011) 19–44.
[38] S. Libertino, V. Aiello, A. Scandurra, M. Renis, F. Sinatra, Immobilization of the enzyme glucose oxidase on both bulk and porous SiO_2 surfaces, Sensors 8 (9) (2008) 5637–5648.
[39] S.A. Dougherty, J. Liang, T.F. Kowalik, Template-assisted fabrication of protein nanocapsules, J. Nanopart. Res. 11 (2) (2008) 385–394.
[40] J. Shao, C. Wen, M. Xuan, H. Zhang, J. Frueh, M. Wan, L. Gao, Q. He, Polyelectrolyte multilayer-cushioned fluid lipid bilayers: a parachute model, Phys. Chem. Chem. Phys. 19 (3) (2017) 2008–2016.
[41] D. Yoo, S.S. Shiratori, M.F. Rubner, Controlling bilayer composition and surface wettability of sequentially adsorbed multilayers of weak polyelectrolytes, Macromolecules 31 (13) (1998) 4309–4318.
[42] I. Delfino, M. Portaccio, B. Della Ventura, D.G. Mita, M. Lepore, Enzyme distribution and secondary structure of sol-gel immobilized glucose oxidase by micro-attenuated total reflection FT-IR spectroscopy, Mater. Sci. Eng. C Mater. Biol. Appl. 33 (1) (2013) 304–310.
[43] J.L.R. Arrondo, F.M. Goñi, Structure and dynamics of membrane proteins as studied by infrared spectroscopy, Prog. Biophys. Mol. Biol. 72 (4) (1999) 367–405.
[44] K. Kohler, P.M. Biesheuvel, R. Weinkamer, H. Mohwald, G.B. Sukhorukov, Salt-induced swelling-to-shrinking transition in polyelectrolyte multilayer capsules, Phys. Rev. Lett. 97 (18) (2006), 188301.
[45] J. Borges, J.F. Mano, Molecular interactions driving the layer-by-layer assembly of multilayers, Chem. Rev. 114 (18) (2014) 8883–8942.
[46] S. Zhang, L. Yang, D. Ding, P. Gao, F. Xia, M.L. Bruening, Highly rectifying fluidic diodes based on asymmetric layer-by-layer nanofilms on nanochannel membranes, Anal. Chem. 93 (9) (2021) 4291–4298.